Journal of Materials Chemistry C

Accepted Manuscript

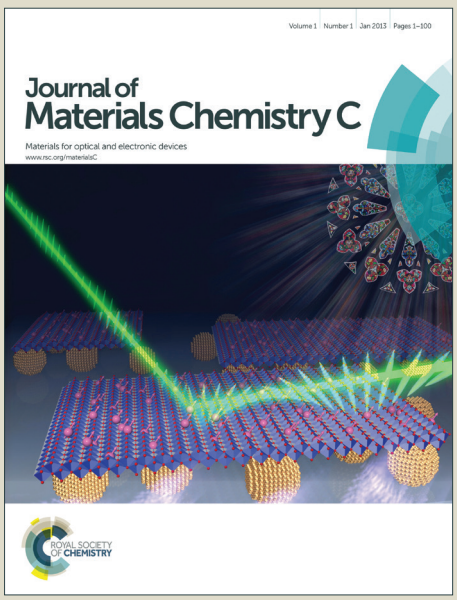

ROYAL SOCIETY OF CHEMISTRY

www.rsc.org/materialsC

Journal Name

RSCPublishing

ARTICLE

Highly efficient orange and deep-red organic light emitting diodes with long operational lifetime using carbazole-quinoline based bipolar host materials

Cite this: DOI: 10.1039/x0xx00000x

Received , xx
Accepted , xx

DOI: 10.1039/x0xx00000x

www.rsc.org/

Chin-Hsien Chen, Lun-Chia Hsu, P. Rajamalli, Yu-Wei Chang, Fang-Iy Wu, Chuang-Yi Liao, Ming-Jai Chiu, Pei-Yu Chou, Min-Jie Huang, Li-Kang Chu and Chien-Hong Cheng*

Orange and deep red-emitting phosphorescent organic light-emitting diodes (PhOLEDs) are important for OLED display and lighting; however, high-performance with long operational lifetime hosts designed for orange/deep red PhOLEDs are very rare. Three new carbazole-quinoline hybrids are synthesized and used as the host materials for orange and deep-red PhOLEDs. These bipolar hosts show high glass transition temperatures 90 ~ 146 °C and triplet energy gaps 2.51 ~ 2.95 eV. The optimized orange PhOLEDs using 9-(4-(4-phenylquinolin-2-yl)phenyl)-9*H*-carbazole (CzPPQ) as the host shows the highest external quantum efficiency (EQE) of 25.6% and a power efficiency of 68.1 lm W^{-1}, which are the highest values for orange PhOLEDs. More importantly, the efficiency roll-off is extremely small for both the orange and deep-red devices. For example, an orange device showed EQE of 25.1% at 100 cd m^{-2} and 23.6% at 1000 cd m^{-2}; the result appears to be the lowest efficiency roll-off for orange PhOLEDs to date. Additionally, the operational lifetime of both the orange and deep-red devices gave T_{50} of more than 26412 and 11450 h, respectively at an initial luminance 500 cd m^{-2}. The values are 12 times (orange) and 6 times (red) longer than those of the corresponding the devices using CBP as the host.

1 Introduction

Organic light-emitting devices (OLEDs) with high efficiency, low power consumption and long operational lifetime are highly needed for application in flat panel displays and lighting.[1] PhOLEDs have drawn immense attention because of the ability of harvesting both singlet and triplet energy for emission.[2] Although deep-red PhOLEDs have been studied considerably, there are still important issues such as triplet-triplet annihilation (TTA) and carrier trapping that should be solved.[3] Orange PhOLEDs are widely employed in white organic light-emitting diodes (WOLEDs) using two phosphorescent emitters.[4] Therefore, high performance orange PhOLEDs are also greatly needed. While efficient orange and deep-red phosphorescent dopants have been well developed,[5] hosts for orange and deep-red PhOLEDs were rarely reported.[6,7] A suitable host material for PhOLEDs should possess high thermal stability and a triplet energy level (T1) higher than that of the emitting phosphors. Besides, a host with bipolar feature is highly desired to achieve high and balanced charge transporting ability.

Recently, several research groups had reported different types of bipolar host materials.[8,9] For example, we demonstrated a universal bipolar host, bis-4-(*N*-carbazolyl)phenyl)phenylphosphine oxide (BCPO) containing a phosphine oxide as the electron acceptor and two carbazole groups as the electron donor for the application to blue, green and red PhOLEDs with high device efficiencies.[9a] We also reported highly efficient deep-red PhOLEDs with long operational lifetime using bis(indoloquinoxalinyl) derivatives as the bipolar hosts.[9b] In general, the bipolar host materials contain an electron-donating and electron-withdrawing moiety for hole and electron transport, respectively. Many bipolar hosts contain a carbazolyl moiety for the hole transporting property and for a large triplet energy gap.[8a-c,f,9,10] Further, the carbazolyl moiety also can improve the thermal and morphology stability because of the rigid structure of the moiety. For electron-withdrawing moieties, phosphine oxide,[9a,11] pyridine,[12] and oxadiazole[13] etc. have been used by several research groups. Unfortunately, these materials are not promising hosts for orange PhOLEDs.

Therefore, it is very important to design suitable host materials for orange electrophosphorescent device to improve both efficiencies and operational lifetimes.

In this paper, we report three carbazole-quinoline based bipolar host materials (Scheme 1) for orange and deep-red phosphorescence devices. We introduced a quinoline moiety as the acceptor and carbazolyl groups as the donor group. The quinoline analogues were used widely in electron transporting layer (ETL) because of the high electron transporting ability and thermal stability.[14] Orange and deep-red PhOLEDs were fabricated using these three materials as the host. A maximum EQE of 25.6% and a power efficiency of 68.1 lm W^{-1} were obtained using 9-(4-(4-phenylquinolin-2-yl)phenyl)-9*H*-carbazole (CzPPQ) as the host. In addition, the device shows the lowest efficiency roll-off for orange PhOLEDs to date with an EQE of 25.1% at 100 cd m^{-2} and 23.6% at 1000 cd m^{-2}, respectively. These compounds are also excellent host materials for iridium deep-red phosphor device and depict low efficiency roll-off. In addition, both the orange and deep-red devices show very long operational lifetimes of more than 26412 and 11450 h at T_{50}, respectively at an initial luminance 500 cd m^{-2}. This is 12 times (orange) and 6 times (red) higher than the corresponding CBP-based device. To the best of our knowledge, the efficiency and operational lifetime of the orange device are the highest values reported to date.

2 Result and discussions

2.1 Synthesis and characterization

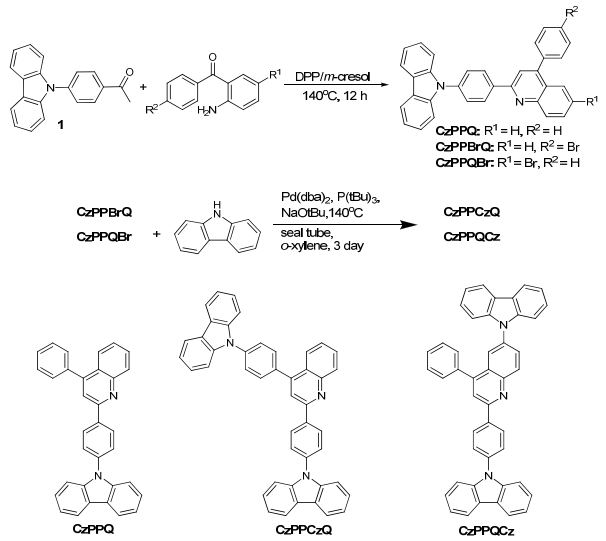

Scheme 1 Synthesis and chemical structures of the **CzPPQ** analogues.

As shown in Scheme 1, CzPPQ was readily prepared from an acid-catalyzed Friedländer reaction of 1-(4-(9*H*-carbazol-9-yl)phenyl)ethanone (1) with 2-aminobenzophenone in high yield using diphenyl phosphate (DPP) as the acid.[15] Similar reaction conditions were employed to prepare the bromo derivatives of CzPPQ 9-(4-(6-bromo-4-phenylquinolin-2-yl)phenyl)-9*H*-carbazole (CzPPQBr) and 9-(4-(4-(4-bromophenyl)quinolin-2-yl)phenyl)-9*H*-carbazole (CzPPBrQ) from 1 and the corresponding substituted 2-aminobenzophenones. CzPPQBr and CzPPBrQ were then further treated with carbazole to give the final carbazolyl phenyl quinolines derivatives CzPPQCz and CzPPCzQ, respectively, via the Pd-catalyzed C-N coupling reaction.[16] The initial ketone **1** was obtained according to the procedures reported in the literature.[17] The detailed preparation procedures for the intermediates and final compounds are given in the experimental section. These derivatives were characterized by ^{1}H and ^{13}C NMR spectral data, high-resolution mass (HRMS) and elemental analysis data. These host materials were further purified by repeated temperature gradient vacuum sublimation before fabrication.

2.2 Photophysical properties

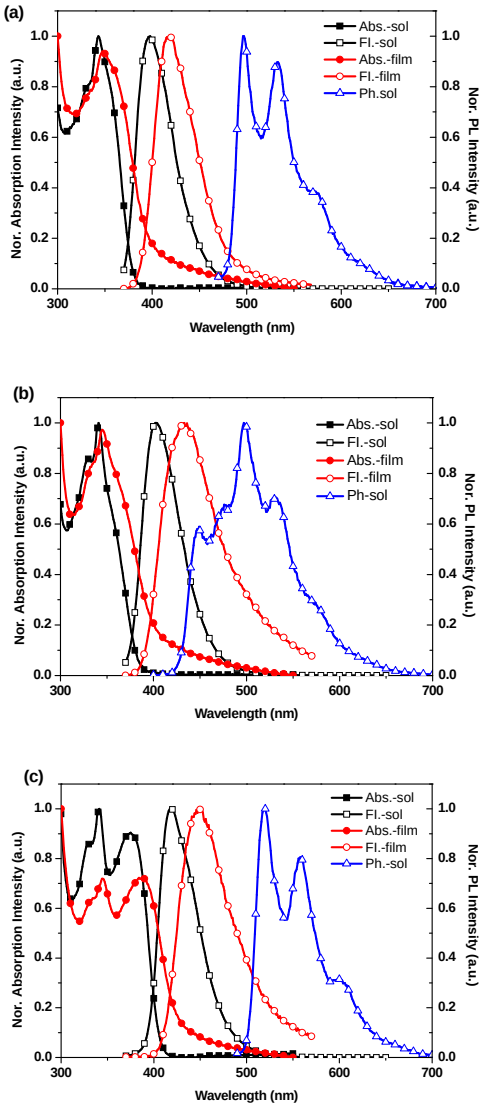

Fig.1 The absorption and fluorescence (λ_{ex} 345 nm) spectra of (a) **CzPPQ**, (b) **CzPPCzQ** and (c) **CzPPQCz** in toluene solution (10^{-5} M), and neat film measured at RT and the phosphorescence spectraof these compounds measured in 2-methyltetrahydrofuran (10^{-5} M) at 77 K.

Table 1 Physical and thermal properties of CzPPQ, CzPPCzQ and CzPPQCz

Host	$\lambda_{abs\ max}$[a] (nm)	λ_{em}[a] (nm) at 300 K	λ_{em}[b] (nm) at 300 K	T_g[c] (°C)	T_d[d] (°C)	HOMO[e] (eV)	LUMO[f] (eV)	E_g[g] (eV)	E_T[h]
CzPPQ	343	397	418	90	345	5.77	2.45	3.32	2.61
CzPPCzQ	341	402	433	145	419	5.79	2.50	3.29	2.95
CzPPQCz	341, 374	419	448	138	421	5.83	2.71	3.12	2.51

[a] 10^{-5} M Toluene solution. [b] 50-nm Thin film. [c] Obtained from DSC measurements. [d] Obtained from TGA measurements. [e] Measured from the oxidation potentials in 10^{-3} M DMF solution by cyclic voltammetry. [f] HOMO - E_g. [g] Estimated from the optical absorption threshold. [h] Estimated from the onset of phosphorescence spectra.

Fig. 1 shows the UV-vis absorption and photoluminescence spectra of CzPPQ, CzPPCzQ and **C**zPPQCz in solution and thin film. As revealed in Fig. 1a, the absorption maximum of CzPPQ in toluene appears at 343 nm assigned as the π-π* transition of the molecule;[18] the emission peak appears at 397 nm (10^{-5} M) and showed slightly red-shift as the concentration increases. As expected, the emission band of the CzPPQ in thin film red-shifted substantially (21 nm) probably due to the relatively large intermolecular interaction in the thin film. Fig. 1a also displays the phosphorescence spectrum of CzPPQ in 2-methyltetrahydrofuran solution at 77 K; the triplet energy gap (E_T) was calculated to be 2.61 eV. The UV-vis absorption and photoluminescence (PL) spectra of CzPPCzQ and CzPPQCz are displayed in Fig. 1b and 1c. From these spectra, the absorption maxima, emission maxima, singlet and triplet energy gaps of these molecules were obtained and are listed in Table 1. The results in Table 1 indicate that the singlet energy gap of these three molecules decreases in the order CzPPQ > CzPPCzQ > CzPPQCz as expected based on the conjugation of the molecules. On the other hand, the order for the triplet energy gap follows the sequence CzPPCzQ > CzPPQ > CzPPQCz. The phosphorescence spectrum patterns of CzPPQ and CzPPQCz are similar, although the energy is different. On the other hand, the phosphorescence spectrum of CzPPCzQ is showing peaks in high energy region leading to the relative high triplet gap of CzPPCzQ (see Table 1). To gain more insight into the photophysical properties, we also studied the solvent effect on the absorption and emission spectra of these materials. As revealed in Fig. S1 the solvent polarity affects substantially the emission wavelength and the band width, but shows little influence on the absorption spectra. As the polarity of the solvent increases, the PL maximum red shifts and the band width of the emission spectrum increases. For example, the emission peak of CzPPQ in low polar toluene appears at 397 nm and shifts to 465 nm in high polar acetonitrile. In addition, the bandwidth grows from 45 nm in toluene to 88 nm in acetonitrile. Similar effect was also observed for CzPPCzQ and CzPPQCz as shown in Fig. S1.

2.3 Electrochemical properties and thermal properties

The electrochemical behaviors of CzPPQ, CzPPCzQ and CzPPQCz were investigated by cyclic voltammetry (CV) and the results were shown in Fig. S2. All of the three compounds displayed quasi-reversible reduction waves with onset potentials at -2.19~-2.29 V (*vs.* Fc/Fc^+). On the other hand, the onset potentials of their oxidation waves are 0.97~1.03 V (*vs.* Fc/Fc^+). The highest occupied molecular orbital (HOMO) energy levels were calculated to be 5.77~5.83 eV based on the oxidation potentials and the ionization potential (4.8 eV) of Fc/Fc^+. The lowest unoccupied molecular orbital (LUMO) energy level were calculated to be 2.45~2.71 eV from HOMO and E_g. The irreversible oxidation potential at 0.97~1.03 V for all these three compounds are likely due to the one electron oxidation of a carbazolyl group to form a cationic radical.[19] In the reduction CV, all CzPPQ's analogues reveal a quasi-reversible peak potential at ca. 2.25 V suggesting that the quinoline moiety in these compounds undergoes one electron reduction at the potential.[20]

To seek further support of the bipolar nature and to gain insight into the electronic states of these materials, density functional theory (DFT) calculation for these materials was performed. The results (Fig. 2) reveal that the HOMO of CzPPQ is distributed mostly over the carbazolyl phenyl groups. On the other hand, its LUMO is localized mainly on the quinoline group and to less extent on the attached phenyl and phenylene groups. These results are consistent with the electrochemical studies that the oxidation is mainly on the

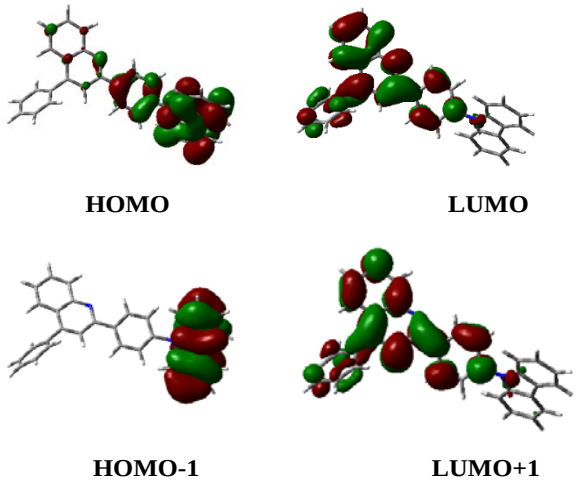

Fig. 2 Calculated electron contour plots of the occupied and unoccupied molecular orbitals of CzPPQ.

Table 2 EL performances of the devices with **CzPPQ**, **CzPPCzQ** and **CzPPQCz** as host

Device[a]	Host	V_d[b] [V]	L_{max}[c] [cd m^{-2}, V]	EQE$_{max}$[c] [%, V]	CE$_{max}$[c] [cd A^{-1}]	PE$_{max}$[c] [lmW^{-1}]	λ_{max}[c] [nm] at 8V	CIE at 8V (x, y)
O1	CzPPQ	3.0	129885, 14.5	25.6, 3.5	75.8, 3.5	68.1, 3.5	580	0.55, 0.45
O2	CzPPCzQ	3.0	144746, 16.5	21.6, 3.5	59.4, 3.5	53.4, 3.5	586	0.56, 0.44
O3	CzPPQCz	2.7	120274, 17.0	17.2, 4.0	51.2, 4.0	50.1, 3.0	582	0.55, 0.45
R1	CzPPQ	2.9	61485, 15.5	19.3, 4.0	24.8, 4.0	24.4, 3.0	620	0.67, 0.33
R2	CzPPCzQ	3.1	65867, 15.5	19.4, 4.0	24.4, 5.0	20.5, 3.5	620	0.67, 0.33
R3	CzPPQCz	3.0	68384, 16.5	21.4, 5.0	27.5, 4.5	24.1, 3.5	620	0.67, 0.33

[a] Device configuration: ITO/NPB (20 nm)/TCTA (10 nm)/host: dopant (4 wt %) (30 nm)/BCP (15 nm)/Alq_3 (50 nm)/LiF (1 nm)/Al (100nm); [b] V_d, The operating voltage at a brightness of 1 cd m^{-2}; [c] L_{max} , Maximum luminance; EQE$_{max}$, Maximum external quantum efficiency; CE$_{max}$, Maximum current efficiency; PE$_{max}$, Maximum power efficiency; and λ_{max}, The wavelength where the EL spectrum having the maximum intensity

carbazole groups and the reduction is on the quinoline group of the CzPPQ molecule. The HOMO and LUMO of CzPPCzQ are similar to those of CzPPQ. The extra carbazolyl group in CzPPCzQ does not appear in the HOMO, but appears in HOMO-1 (Fig. S3). On the other hand, the results of DFT calculation of CzPPQCz show that its HOMO is on the two carbazolylphenyl moieties and the LUMO is on the quinoline and the attached phenylene groups. Overall, the DFT calculation is consistent with the results of the CV studies and supports the bipolar nature of these host materials.[21a-c]

The thermal properties of these materials were investigated by differential scanning calorimetry (DSC) and thermogravimetric analysis (TGA) and the results are summarized in Table 1. The glass transition temperatures (T_gs) of CzPPQ, CzPPCzQ and CzPPQCz appear at 90, 145 and 138 °C, respectively. The observed higher T_gs for CzPPCzQ and CzPPQCz is presumably due to the presence of an extra carbazolyl group on the molecules. In addition, no crystallization and melting point were detected for these three compounds in the second heating. All the compounds show high decomposition temperatures (T_d) 345 ~ 421°C.

2.4 Electrophosphorescent devices

To examine the carrier transporting properties of these materials, we fabricated the hole-only and electron-only devices of CzPPQ, CzPPCzQ and CzPPQCz. The hole only device consists of the layers ITO/NPB (10 nm) /TCTA (5 nm)/host (30 nm)/NPB (15 nm)/Al (100 nm), while the electron-only devices has the configuration ITO/BCP (15 nm)/host (30 nm)/BCP (15 nm)/LiF (1 nm)/Al (100 nm), where NPB = (4,4'-bis[*N*-(1-naphthyl)-*N*-phenylamino]biphenyl, TCTA = (4,4',4''-tri(*N*-carbazolyl)triphenylamine and BCP = 2,9-dimethyl-4,7-diphenyl-1,10-phenanthroline. The NPB and BCP layers were used to prevent electron and hole injection from the cathode and the anode, respectively. Current density versus voltage characteristics of the electron-only and hole-only devices are shown in Fig.3 and Fig. S4. The order of hole and electron current density was CzPPQ > CzPPQCz > CzPPCzQ. As shown in Fig. 3, the current density versus voltage (I – V) curves for the CzPPQ-based hole-only and electron-only devices are close to each other. This observation indicates that CzPPQ is both a good electron and hole transporting material and is bipolar in nature. Further, single carrier devices of CzPPQ, CzPPCzQ and CzPPQCz were fabricated and the carrier mobilities were determined by SCLC (space charge limited current) method.[21d,e] The results are shown in Fig. S5 and summarized in Table S1. As shown in the table, the hole (2.13 x 10^{-6} cm^2/Vs) and electron (1.18 x 10^{-6} cm^2/Vs) mobilities of CzPPQ are much closer than those of the other two hosts. The results suggest that CzPPQ has better balanced hole/electron injection and transport properties compared to CzPPQCz and CzPPCzQ. For the latter two species, their hole mobilities are higher than their electron mobilities due to the presence of two hole transporting carbazole units compared to only one electron transporting quinolone unit in the molecules.

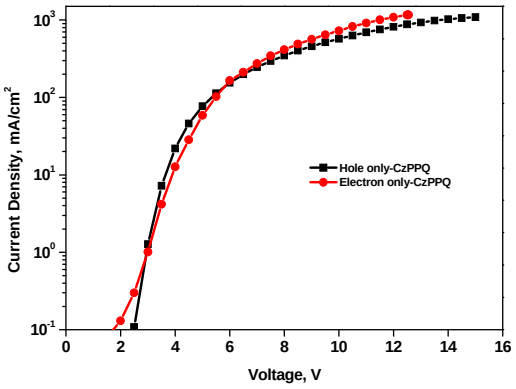

Fig. 3 Current density versus voltage for the hole-only and electron-only devices.

We next examine the energy transfer properties of these three carbazole-quinoline based materials, particularly the energy transfer to a phosphorescent dopant. Thus, the films of CzPPQ, CzPPCzQ and CzPPQCz doped with 4% of $Ir(pq)_3$ (tris(2-phenylquinoline)iridium(III)) were made by vapor deposition. The quantum yields of these films excited at 330 nm were 67%, 40% and 34%, respectively. It is noteworthy that the observed quantum yields are parallel to the OLED efficiencies using these

doped films as the emitting layers (see Table 2, devices O1-O3). Further, to see the effect of these three materials on the phosphorescent lifetime of the doped orange and red iridium complexes ($Ir(pq)_3$) and red ($Ir(piq)_3$, the transient PL decay of the $Ir(pq)_3$-doped and $Ir(pq)_3$-doped thin films were measured. As shown in Fig. S6, the $Ir(pq)_3$-doped films exhibit nearly mono-exponential decay with lifetimes between 1.03 and 1.40 μs (Table S2). Similarly, the $Ir(piq)_3$-doped films also exhibit nearly mono-exponential decay with lifetimes between 0.98 and 1.18 μs (Fig. S7 and Table S2). The lifetime for the two iridium complexes in the three carbazole-quinoline-based thin films appears to follow the order: CzPPQ > CzPPCzQ > CzPPQCz, although the difference is quite small.

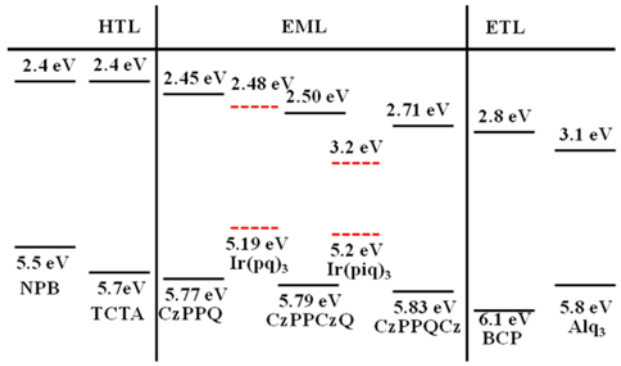

Fig. 4 The HOMO/LUMO levels of the materials used in the EL devices.

To know the performance of CzPPQ, CzPPCzQ and CzPPQCz as hosts for phosphorescence organic light-emitting devices (PhOLEDs), we fabricated several orange and deep-red PhOLEDs using these materials as the hosts. With the triplet energy gaps higher than 2.5 eV, these materials appear to be ideal host materials for orange and red PhOLEDs. Tris(2-phenylquinoline)iridium(III) ($Ir(pq)_3$) was chosen as the orange dopant for the orange PhOLEDs. The optimized device configuration consisting of ITO (indium tin oxide)/NPB (20 nm)/TCTA (10 nm)/CzPPQ: 4 wt% dopant (30 nm)/BCP (15 nm)/Alq_3 (50 nm)/LiF (1 nm)/Al (100 nm). Devices O1-O3 were fabricated using CzPPQ, CzPPCzQ and CzPPQCz as the host, respectively. The performance of these devices is summarized in Table 2, while the relative energy levels of these materials are displayed in Fig. 4. The electroluminescence spectra of these devices are shown in Fig. S8 and no emission from neighboring materials were observed for all these devices. This result suggests that holes and electrons are completely confined within the EML and recombination of the charge carriers takes place only in the emitting layer (EML). Fig. 5a provides the current-voltage-luminance (I-V-L) characteristics and Fig. 5b shows the external quantum efficiencies vs luminance of devices O1-O3. The results indicate that device O1 hosted by CzPPQ gave the highest EQE, current efficiency and power efficiency achieving an EQE of 25.6%, current efficiency of 75.8 cd A^{-1} and power efficiency of 68.1 lm W^{-1}, higher than the corresponding values given by devices O2 and O3 hosted by CzPPCzQ (EQE = 21.6%) and CzPPQCz (17.2%), respectively (Table 2 and Fig. S9). The EQEs of orange PhOLEDs with single hosts are rarely higher than 20% and their power efficiency are generally low, much lagging behind the co-host orange devices.[22]

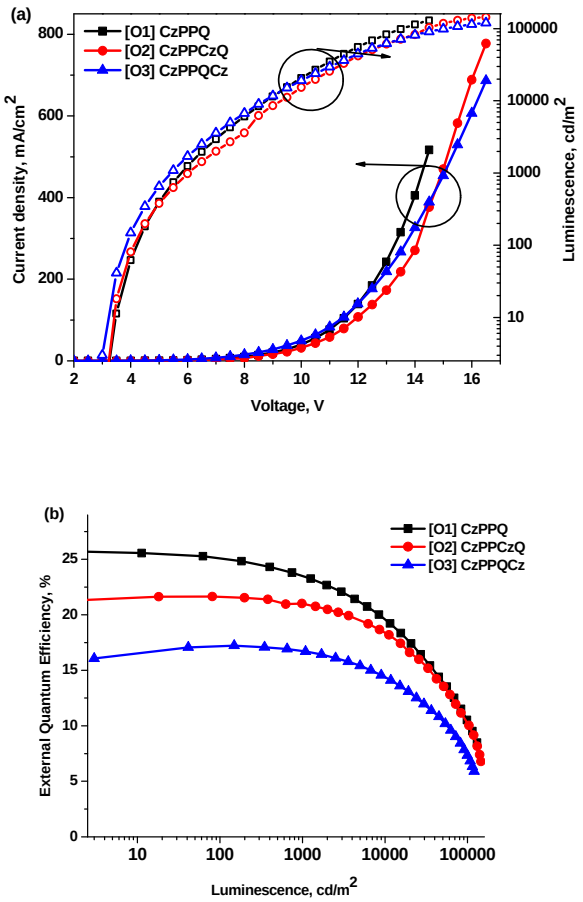

Fig. 5 (a) Current density-voltage-luminescence (*I* – *V* – *L*) characteristics and (b) EQE- luminance curves for 4 wt% $Ir(pq)_3$-based devices with CzPPQ, CzPPCzQ and CzPPQCz as the host materials in the EML.

In this work, the EQE and the power efficiency of the device hosted by CzPPQ are the highest one for the orange devices to the best of our knowledge and even higher than the co-host device.[22] The low operation voltage and the high EQE renders the devices with high power efficiency. The bipolar property and balanced charge transporting properties of CzPPQ likely account for the excellent performance of devices O1-O3. More importantly, all the devices show very small roll-off. The smallest efficiency roll-off was observed device O1 hosted by CzPPQ, with an EQE of 25.1% at 100 cd m^{-2} and 23.6% at 1000 cd m^{-2}. This is the smallest efficiency roll-off for single host orange PhOLEDs to date. The small efficiency roll-off is likely due to the wide charge recombination zone and the charge balance in the EMLs even at higher current density resulting from the bipolar feature of the hosts. It is expected that triplet-triplet annihilation of the iridium dopants takes place easily in a narrow recombination zone in the EML.[23] Among the three host materials, CzPPQ shows the best performance for orange

PhOLEDs. We accounted the best performance of CzPPQ based device to the well matched energy levels (Fig. 4) and balanced charge injection along with high PL quantum yield in the CzPPQ thin film.

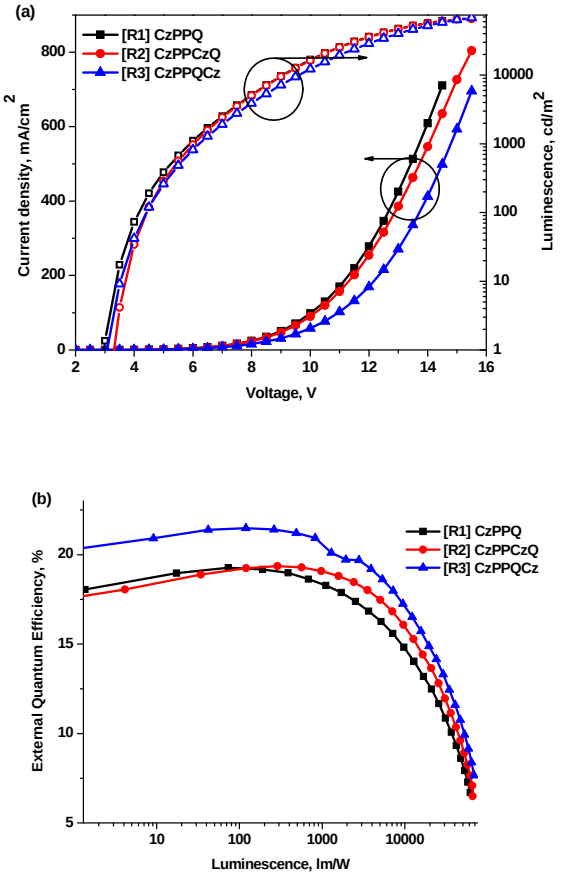

Fig. 6 (a) Current density-voltage-luminescence (*I–V–L*) characteristics and (b) EQE-luminancecurves for 4 wt% Ir(piq)$_3$-based devices with CzPPQ, CzPPCzQ and CzPPQCz as the host materials.

Besides, to see the capability of these three host materials for deep-red devices, R1-R3 using Ir(piq)$_3$ as the dopant and CzPPQ, CzPPCzQ and CzPPQCz as the host, respectively, were fabricated. The structures of these devices are the same as that of devices O1-O3 except the dopant in the emission layer. The I-V-L characteristics, external quantum efficiencies vs luminance of these devices are shown in Fig. 6, while the performance data are listed in Table 2. Device R3 shows a low turn-on voltage of 3.0 V and maximum external quantum efficiency, current efficiency and power efficiency of 21.4%, 27.5 cd A^{-1} and 24.1 lm W^{-1}, respectively. Devices R1 and R2 also give EQE of 19.3% and 19.4%, respectively. From the electroluminescence spectra of these devices in Fig. S10, only the emission of Ir(piq)$_3$ can be seen, indicating that the hole and electron recombination occurs only in the EML. Furthermore, devices R1-R3 also show very small roll-off. For example, device R3 retains an EQE over 20% even at 1000 cd m^{-2}.

2.5 Operational lifetime

Finally, to see the potential of these high performance CzPPQ-based devices for industrial application, we measured the operational lifetimes (T_{50}) of these devices. For comparison, devices using conventional CBP as the host were also fabricated for the lifetime measurements. Fig. 7 shows the plots of relative brightness L/L_0 vs time for these four devices operated at constant current density of 10 mA cm^{-2}. At this current density, device O1 consisting of CzPPQ and Ir(pq)$_3$ in the emission layer exhibits an initial brightness of 5522 cd m^{-2}. The half-lifetime of a device at different initial luminance value can be calculated from the experimental *L–t* curve and with eq (1).

$$L_0^n \times T_{50} = \text{constant} \qquad (1)$$

Where L_0 is the initial luminance, T_{50} is the half lifetime for the luminance decay and n is the accelerated factor which is assumed to be 1.5.[9b,24] Based on the results of the *L–t* curves (Fig. 7) and eqn (1), we estimated the lifetime of the devices at 500 cd m^{-2}.

Interestingly, the operational lifetime (T_{50}) for device O1 at an initial luminance 500 cd m^{-2} is estimated to be 26412 h. A comparison of the plots for O1 and the CBP-based device suggests that the lifetime of device O1 is ca 12 times longer than that of the CBP-based device. In addition, device R1 consisting of CzPPQ and Ir(piq)$_3$ in the emission layer (EML) exhibits an initial brightness of 11402 cd m^{-2} at constant current density of 10 mA cm^{-2}. Similar to that of orange device O1, R1 also shows a long operational lifetime as compared to the corresponding CBP-based device. The operational lifetime (T_{50}) of device R1 at an initial luminance of 500 cd m^{-2} is estimated to be 11450 h, approximately 6 times longer than that of the CBP-based device. The reason for long lifetime of the (O1 and R1) devices could be due to higher glass transition temperature (T_g) of CzPPQ and the balanced charge injection and wide recombination zone in the EML of the CzPPQ-based devices.

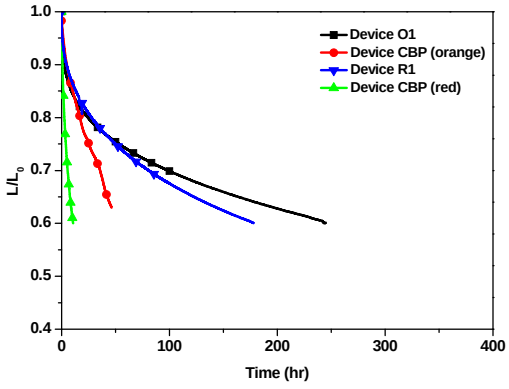

Fig. 7 Comparison of device operational stability for devices O1 (L_0= 5522 cd m^{-2}), CBP-orange (L_0= 5488 cd m^{-2}), R1 (L_0= 11402 cd m^{-2}), and CBP-red (L_0= 11295 cd m^{-2}) under a constant operating current density of 10 mA cm^{-2} under a nitrogen atmosphere in a glove box.

3 Conclusions

We have successfully developed a new strategy for the preparation of bipolar host materials based on a central quinoline as the electron- accepting group and carbazole(s) as the electron donor center. Three of these bipolar materials CzPPQ, CzPPCzQ and CzPPQCz were thus synthesized and characterized. The bipolar property of these materials is supported by the CV measurements, DFT calculation and the I-V curves of the electron-only and hole-only devices. The use of these three materials as the host materials for orange and deep-red EL devices showed excellent device performances with the highest EQE of 25.6% and power efficiency of 68.1 lm W^{-1}. In addition, these devices show negligible roll-off; the EQE for O1 at 1000 cd m^{-2} maintains 92% of its maximum value. The operational lifetime (T_{50}) measurement of the CzPPQ-based devices O1 and R1 give operational lifetime (T_{50}) of 26412 and 11450 h at a brightness of 500 cd m^{-2}, respectively, much longer than those of the devices using CBP as the host.

4 Experimental sections

4.1 General information

1-(4-(9*H*-Carbazol-9-yl)phenyl)ethanone (1) was synthesized using a reported method.[17] Other reagents and solvents were used as purchased without further purification unless otherwise stated. ^{1}H and ^{13}C NMR spectra were recorded with a Varian Mercury 400 spectrometer. The HRMS spectra were recorded on a Finnigan MAT-95XL mass spectrometer. The glass transition temperatures of compounds were determined by DSC under nitrogen atmosphere using a DSC-Q10 instrument. The decomposition temperature corresponding to 5% weight loss was conducted on a Perkin-Elmer Pyris 1 TGA thermal analyzer. UV-vis spectra were recorded on a Hitachi U-3300 spectrophotometer and PL spectra were measured using a Hitachi F-4500 fluorescence spectrophotometer. Cyclic voltammetry (CV) measurements were performed on a CH Instruments 600A electrochemical analyzer. The reduction and oxidation measurements were recorded using a Pt wire as counter electrode, a graphite electrode as the working electrode and a Ag/Ag^+ (0.01 M $AgNO_3$) as the reference electrode, respectively, in anhydrous DMF solution containing 0.10 M $(TBA)PF_6$ as the supporting electrolyte. By assuming that the ferrocene/ferrocenium (Fc/Fc^+) couple is 4.8 eV below the vacuum level, the onset oxidation potentials versus Fc/Fc^+ of each complex were used to calculate the HOMO energy levels. The molecular geometry optimizations and electronic properties were computed by carrying out the Gaussian 03 program with density functional theory (DFT) and time-dependent DFT (TDDFT) calculations, in which the Becke's three-parameter functional combined with Lee, Yang, and Parr's correlation functional (B3LYP) hybrid exchange-correlation functional with the 6-31G* basic set were used. The molecular orbitals were visualized on the Gaussview 4.1 software.

4.2 Synthesis of 9-(4-(4-phenylquinolin-2-yl)phenyl)-9*H*-carbazole (CzPPQ)

A mixture of 1-(4-(9*H*-carbazol-9-yl)phenyl)ethanone (285 mg, 1.00 mmol), 2-aminobenzophenone (400 mg, 2.00 mmol), diphenyl phosphate (DPP) (751 mg, 3.00 mmol) and freshly distilled *m*-cresol (1.0 mL) was heated under nitrogen atmosphere at 140 °C for 12 h. After cooling, the reaction mixture was added to a solution of 10% (v/v) triethylamine in methanol (10.0 mL). The precipitated product was purified by column chromatography (hexane/EtOAc, 10:1) to yield CzPPQ (381 mg, 85.4%). ^{1}H NMR (400 MHz, $CDCl_3$, δ): 7.31 (dd, 2H, J = 7.6, 7.2 Hz), 7.44 (dd, 2H, J = 8.0, 7.6 Hz), 7.50-7.62 (m, 8H), 7.73-7.80 (m, 3H), 7.91 (s, 1H), 7.95 (d, 1H, J = 8.4 Hz), 8.16 (d, 2H, J = 7.6 Hz), 8.30 (d, 1H, J = 8.4 Hz), 8.43 (d, 2H, J = 8.4 Hz); ^{13}C NMR (100 MHz, $CDCl_3$, δ): 109.8, 119.1, 120.1, 120.3, 123.5, 125.7, 125.8, 126.0, 126.5, 127.2, 128.5, 128.6, 129.0, 129.5, 129.7, 130.1, 138.2, 138.5, 138.7, 140.6, 148.8, 149.4, 155.9; HRMS (EI, m/z): [M^+] calcd for $C_{33}H_{22}N_2$, 446.1783; found, 446.1779. Anal. calcd. for $C_{33}H_{22}N_2$: C 88.76, H 4.97, N 6.27; found: C 88.49, H 4.87, N 6.35.

4.3 Synthesis of 9,9'-(quinoline-2,4-diylbis(4,1-phenylene))-bis(9*H*-carbazole) (CzPPCzQ)

To a sealed tube consisting of 9-(4-(4-(4-bromophenyl)quinolin-2-yl)phenyl)-9*H*-carbazole (CzPPBrQ) (525 mg, 1.00 mmol), carbazole (200 mg, 1.2 mmol) and $Pd(dba)_2$ (33 mg, 0.060 mmol) were added tri-*tert*-butylphosphine (96 mg, 0.048 mmol), sodium *tert*-butoxide (432 mg, 4.50 mmol) and then *o*-xylene (3.00 mL) via a syringe in a nitrogen box. The reaction mixture was heated and stirred at 150 °C for 48 h. The reaction mixture was then cooled to room temperature, filtered through a Celite pad, and the latter was washed with dichloromethane. After concentration of the filtrate followed by washing of the brown solid with dichloromethane, the product was purified by column chromatography (hexane/EtOAc, 10:1) to yield CzPPCzQ (528 mg, 86.3%). ^{1}H NMR (400 MHz, $CDCl_3$, δ): 7.29-7.35 (m, 3H), 7.42-7.52 (m, 7H), 7.57-7.62 (m, 3H), 7.75-7.86 (m, 7H), 8.00 (s, 1H), 8.09 (d, 1H, J = 8 Hz), 8.17 (t, 4H, J = 8 Hz), 8.33 (d, 1H, J = 8 Hz), 8.48 (d, 2H, J = 8.8 Hz); ^{13}C NMR (100 MHz, $CDCl_3$, δ): 109.5, 109.8, 120.0, 120.2, 120.3, 120.3, 120.4, 123.1, 123.5, 123.6, 126.0, 126.1, 126.6, 127.2, 128.9, 129.2, 129.3, 131.7, 135.8, 137.5, 139.2, 140.6, 140.7, 156.2; HRMS (EI, m/z): [M^+] calcd for $C_{45}H_{29}N_3$, 611.2361; found, 611.2365. Anal. calcd. for $C_{45}H_{29}N_3$: C 88.35, H 4.78, N 6.87; found: C 88.15, H 4.74, N 7.02.

4.4 Synthesis of 9-(4-(6-(9*H*-carbazol-9-yl)-4-phenylquinolin-2-yl)phenyl)-9*H*-carbazole) (CzPPQCz)

To a sealed tube consisting of 9-(4-(6-bromo-4-phenylquinolin-2-yl)phenyl)-9*H*-carbazole (CzPPQBr) (525 mg, 1.00 mmol), carbazole (200 mg, 1.2 mmol) and $Pd(dba)_2$ (0.033 g, 0.060 mmol) were added tri-*tert*-butylphosphine (0.096 g, 0.048 mmol), sodium *tert*-butoxide (0.432 g, 4.50 mmol) and then *o*-xylene (3.00 mL) via a syringe in a nitrogen box. The reaction mixture was heated and stirred at 150 °C for 48 h. The reaction mixture

was then cooled to room temperature, filtered through a Celite pad, and the latter was washed with dichloromethane. After concentration of the filtrate followed by washing of the brown solid with dichloromethane, the product was purified by column chromatography (hexane/EtOAc, 10:1) to yield CzPPQCz (524 mg, 85.7%). ^{1}H NMR (400 MHz, $CDCl_3$, δ): 7.28-7.33 (m, 4H), 7.39-7.46 (m, 7H), 7.51 (t, 4H, J = 8 Hz), 7.61 (d, 2H, J = 7.2 Hz), 7.78 (d, 2H, J = 8.4), 7.96 (dd, 1H, J = 8.0, 2 Hz), 8.00 (s, 1H), 8.11-8.17 (m, 5H), 8.47-8.50 (m, 3H); ^{13}C NMR (100 MHz, $CDCl_3$, δ): 109.7, 109.8, 119.3, 120.1, 120.3, 120.4, 120.5, 123.5, 123.6, 125.5, 125.7, 126.0, 126.1, 126.8, 127.1, 127.3, 129.1, 139.9, 130.0, 131.1, 137.2, 138.1, 138.5, 138.9, 140.7, 148.5, 149.0, 156.0; HRMS (EI, m/z): [M^+] calcd for $C_{45}H_{29}N_3$, 611.2361; found, 611.2367. Anal. calcd. for $C_{45}H_{29}N_3$: C 88.35, H 4.78, N 6.87; found: C 88.25, H 4.96, N 6.54.

4.5 OLEDs fabrication and measurement

Organic chemicals used for fabricating devices were purified by temperature gradient vacuum sublimation. The EL devices were fabricated by vacuum deposition of the materials at a base pressure less than 10^{-6} Torr onto a glass pre-coated with a layer of ITO with a sheet resistance of 25 Ω/square. The deposition rate for organic compounds is 0.5~3 Å s^{-1}. The cathode consisting of LiF/Al was deposited by evaporation of LiF with a deposition rate of 0.1 Å s^{-1} and then by evaporation of Al metal with a rate of 3~10 Å s^{-1}. The active area of the devices is 9 mm^2. The EL spectra were taken with a Hitachi F-4500 fluorescence spectrophotometer. The measurements of current, voltage and luminance were made simultaneously in the air using a Keithley 2400 source meter and a Topcon BM-7 luminance meter. The external quantum efficiencies of the prepared devices were calculated from the EL spectrum, luminance and current density.

Acknowledgements

We thank Ministry of Science and Technology of Republic of China (NSC 100-2119-M-007-010-MY3 and NSC 102-2633-M-007-002) for support of this research and the National Center for High-Performance Computing (Account number: u32chc04) for providing computing time.

Notes and references

Department of Chemistry, National Tsing Hua University, Hsinchu 30013, Taiwan, Fax: 886-3-572469, Tel: 886-3-5721454. E-mail: chcheng@mx.nthu.edu.tw

† Electronic Supplementary Information (ESI) available: Synthesis, optical spectra, CV, DFT calculation, Luminescence vs current efficiency, Luminescence vs power efficiency and electroluminescent spectra. See DOI: 10.1039/b000000x/

1 (a) G. M. Farinola and R. Ragni, *Chem. Soc. Rev.*, 2011, **40**, 3467; (b) U. Mitschke and P. Bauerle, *J. Mater. Chem*., 2000, **10**, 1471; (c) H.-H. Chou, Y.-H. Chen, H.-P. Hsu, W.-H. Chang, Y.-H. Chen and C.-H. Cheng, *Adv. Mater.*, 2012, **24**, 5867; (d) M. A. Baldo, M. E. Thompson and S. R. Forrest, *Nature*, 2000, **403**, 750; (e) A. C. Grimsdale, K. L. Chan, R. E. Martin, P. G. Jokisz and A. B. Holmes, *Chem. Rev.*, 2009, **109**, 897; (f) H. Uoyama, K. Goushi, K Shizu, H. Nomura and C. Adachi, *Nature*, 2012, **492**, 234.

2 (a) Y. Sun, N. C. Giebink, H. Kanno, B. Ma, M. E. Thompson and S. R. Forrest, *Nature*, 2006, **440**, 908; (b) S. Reineke, F. Lindner, G. Schwartz, N. Seidler, K. Walzer, B. Lussem and K. Leo, *Nature*, 2009, **459**, 234; (c) K.-Y. Lu, H.-H. Chou, C.-H. Hsieh, Y.-H. O. Yang, H.-R. Tsai, H.-Y. Tsai, L.-C. Hsu, C.-Y. Chen, I-C. Chen and C.-H. Cheng, *Adv. Mater.*, 2011, **23**, 4933; (d) C.-H. Chen, F.-I. Wu, Y.-Y. Tsai and C.-H. Cheng, *Adv. Funct. Mater.*, 2011, **21**, 3150; (e) H. Sasabe, J.-i. Takamatsu, T. Motoyama, S. Watanabe, G. Wagenblast, N. Langer, O. Molt, E. Fuchs, C. Lennartz and J. Kido, *Adv. Mater.*, 2010, **22**, 5003; (f) H. Sasabe and J. Kido, *J. Mater. Chem.* C, 2013, **1**, 1699.

3 (a) D. F. O'Brien, M. A. Baldo, M. E. Thompson and S. R. Forrest, *Appl. Phys. Lett.*, 1999, **74**, 442; (b) M. A. Baldo, C. Adachi and S. R. Forrest, *Phys. Rev. B*, 2000, **62**, 10967; (c) B. D. Chin, M. C. Suh, M. -H. Kim, S. T. Lee, H. D. Kim and H. K. Chung, *Appl. Phys. Lett.*, 2005, **86**, 133505; (d) S. Reineke, K. Walzer and K. Leo, *Phys. Rev. B*, 2007, **75**, 125328; (e) H. Z. Siboni and H. Aziza, *Appl. Phys. Lett.*, 2012, **101**, 063502.

4 (a) Y. Chen and D. Ma, *J. Mater. Chem.*, 2012, **22**, 18718; (b) T. Peng, Y. Yang, H. Bi, Y. Liu, Z. Hou and Y. Wang, *J. Mater. Chem.*, 2011, **21**, 3551; (c) X.-K. Liu, C.-J. Zheng, M.-F. Lo, J. Xiao, Z. Chen, C.-L. Liu, C.-S. Lee, M.-K. Fung and X.-H. Zhang, *Chem. Mater.*, 2013, **25**, 4454; (d) H. Wu, G. Zhou, J. Zou, C.-L. Ho, W.-Y. Wong, W. Yang, J. Peng and Y. Cao, *Adv. Mater.*, 2009, **21**, 4181; (e) H.-H. Chou, Y.-K. Li, Y.-H. Chen, C.-C. Chang, C.-Y. Liao and C.-H. Cheng, *ACS Appl. Mater. Interfaces*, 2013, **5**, 6168.

5 (a) R. Wang, D. Liu, H. Ren, T. Zhang, H. Yin, G. Liu and J. Li, *Adv. Mater.*, 2011, **23**, 2823; (b) R. Wang, D. Liu, R. Zhang, L. Denga, J. Li, *J. Mater. Chem.*, 2012, **22**, 1411; (c) C.-L. Ho, W.-Y. Wong, Q. Wang, D. Ma, L. Wang and Z. Lin, *Adv. Funct. Mater.*, 2008, **18**, 928; (d) W.-C. Chang, A. T. Hu, J.-P. Duan, D. K. Rayabarapu and C.-H. Cheng, *J. Organomet. Chem.*, 2004, **689**, 4882; (e) D.-S. Leem, S. O. Jung, S.-O. Kim, J.-W. Park, J. W. Kim, Y. -S. Park, Y.-H. Kim, S.-K. Kwon and J.-J. Kim, *J. Mater. Chem.*, 2009, **19**, 8824.

6 X. Yang, H. Huang, B. Pan, M. P. Aldred, S. Zhuang, L. Wang, J. Chen and D. Ma, *J. Phys. Chem. C*, 2012, **116**, 15041.

7 S. Gong, Y. Chen, J. Luo, C. Yang, C. Zhong, J. Qin and D. Ma, *Adv. Funct. Mater.*, 2011, **21**, 1168.

8 (a) E. Mondal, W.-Y. Hung, H.-C. Dai and K.-T. Wong, *Adv. Funct. Mater.*, 2013, **23**, 3096; (b) E. Mondal, W.-Y. Hung, Y.-H. Chen, M.-H. Cheng and K.-T. Wong, *Chem. Eur. J.*, 2013, **19**, 10563; (c) L. Duan, J. Qiao, Y. D. Sun and Y. Qiu, *Adv. Mater.*, 2011, **23**, 1137; (d) Y. T. Tao, C. L. Yang and J. G. Qin, *Chem. Soc. Rev.*, 2011, **40**, 2943; (e) F. -M. Hsu, C. -H. Chien, Y. -J. Hsieh, C. -H. Wu, C. -F. Shu, S. -W. Liu and C. -T. Chen, *J. Mater. Chem.*, 2009, **19**, 8002; (f) W.-Y. Hung, L.-C. Chi, W.-J. Chen, E. Mondal, S.-H. Chou, K.-T. Wong and Y. Chi, *J. Mater. Chem.*, 2011, **21**, 19249.

9 (a) H. -H. Chou and C. -H. Cheng, *Adv. Mater.*, 2010, **22**, 2468; (b) T.-H. Su, C.-H. Fan, Y.-H. Ou-Yang, L.-C. Hsu and C.-H. Cheng, *J. Mater. Chem. C*, 2013, **1**, 5084.

10 (a) H.-H. Chou, H.-H. Shih and C.-H. Cheng, *J. Mater. Chem.*, 2010, **20**, 798; (b) M. -H. Tsai, H. -W. Lin, H. -C. Su, T. -H. Ke, C. Wu, F. -C. Fang, Y. -L. Liao, K. -T. Wong and C. -I. Wu, *Adv. Mater.*, 2006, **18**, 1216.

11 (a) L.-S. Cui, Y. Liu, X.-D. Yuan, Q. Li, Z.-Q. Jiang and L.-S. Liao, *J. Mater. Chem. C*, 2013, **1**, 8177; (b) C. Han, L. Zhu, F. Zhao, Z. Zhang, J. Wang, Z. Deng, H. Xu, J. Li, D. Ma and P. Yan, *Chem. Commun.,* 2014, **50**, 2670; (c) C. Han, Z. Zhang, H. Xu, J. Li, Y. Zhao, P. Yan and S. Liu, *Chem. Eur. J.,* 2013, **19**, 1385.

12 (a) X.-H. Zhao, Z.-S. Zhang, Y. Qian, M.-D. Yi, L.-H. Xie, C.-P. Hu, G.-H. Xie, H. Xu, C.-M. Han, Y. Zhao and W. Huang, *J. Mater. Chem. C*, 2013, **1**, 3482; (b) S. -J. Su, H. Sasabe. T. Takeda and J. Kido, *Chem. Mater.,* 2008, **20**, 1691.

13 S.-H. Cheng, S.-H. Chou, W.-Y. Hung, H.-W. You, Y.-M. Chen, A. Chaskar, Y.-H. Liu and K.-T. Wong, *Organic Electronics*, 2013, **14**, 1086.

14 (a) J. K. Stille, *Macromolecules,* 1981, **14**, 870; (b) A. K. Agrawal and S. A. Jenekhe, *Chem. Mater.,* 1992, **4**, 95; (c) A. K. Agrawal and S. A. Jenekhe, *Macromolecules*, 1993, **26**, 895.

15 L. Lu and S. A. Jenekhe, *Macromolecules*, 2001, **34**, 6249.

16 B. E. Koene, D. E. Loy and M. E. Thompson, *Chem. Mater.,* 1998, **10**, 2235.

17 A. Matsumoto, J. Tanabe, H. Kura, M. Ohwa, (Ciba Specialty Chemicals Holding Inc.) *Switz. WO 2007062963*, 2007.

18 S. A. Jenekhe, L. Lu and M. M. Alam, *Macromolecules*, 2001, **34**, 7315.

19 (a) K. Brunner, A. V. Dijken, H. Bömer, J. J. A. M. Bastiaansen, N. M. M. Kiggen and B. M. W. Langeveld, *J. Am. Chem. Soc.,* 2004, **126**, 6035; (b) J. F. Ambrose, L. L. Carpenter and R. F. Nelson, *J. Electrochem. Soc.,* 1975, **122**, 876.

20 R. Y. Lai, E. F. Fabrizio, L. Lu, S. A. Jenekhe and A. J. Bard, *J. Am. Chem. Soc.,* 2001, **123**, 9112.

21 (a) Y. Tao, Q. Wang, Y. Shang, C. Yang, L. Ao, J. Qin,D. Ma and Z. Shuai, *Chem. Commun.,* 2009, **46**, 77; (b) S. Gong, Y. Chen, C. Yang, C. Zhong, J. Qin and D. Ma, *Adv. Mater.,* 2010, **22**, 5370; (c) W. Jiang, L. Duan, J. Qiao, G. Dong, L. Wang and Y. Qiu, *Org. Lett.,* 2011, **13**, 3146; (d) T. Yasuda, Y. Yamaguchi, D.-C. Zou and T. Tsutsui, *Jpn. J. Appl. Phys.* 2002, **41**, 5626; (e) C. W. Lee and J. Y. Lee, *Chem. Mater.* 2014, **26**, 1616.

22 (a) S. Lee, K. H. Kim, D. Limbach, Y.-S. Park and J.-J. Kim, *Adv. Funct. Mater.,* 2013, **23**, 4105; (b) S. Lee, D. Limbach, K.-H. Kim, S.-J. Yoo, Y.-S. Park and J.-J. Kim, *Organic Electronics*, 2013, **14**, 1856.

23 (a) S. H. Kim, J. Jang, K. S. Yook and J. Y. Lee, *Appl. Phys. Lett.,* 2008, **92**, 023513; (b) M. A. Baldo, C. Adachi and S. R. Forrest, *Phys. Rev. B*, 2000, **62**, 10967.

24 K. Okumoto, H. Kanno, Y. Hamada, H. Takahashi and K. Shibata, *Appl. Phys. Lett.,* 2006, **89**, 13502.

ToC graphics:

Highly efficient orange and deep-red organic light emitting diodes with long operational lifetime using carbazole-quinoline based bipolar host materials

Chin-Hsien Chen, Lun-Chia Hsu, P. Rajamalli, Yu-Wei Chang, Fang-Iy Wu, Chuang-Yi Liao, Ming-Jai Chiu, Pei-Yu Chou, Min-Jie Huang, Li-Kang Chu and Chien-Hong Cheng*

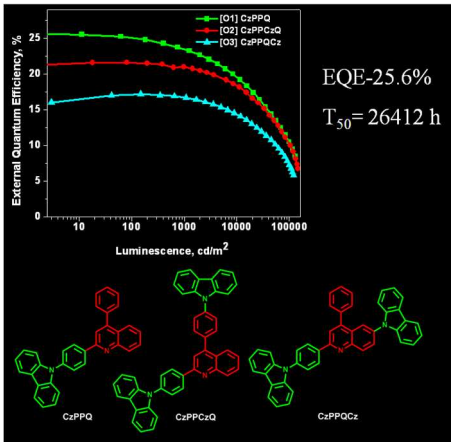

A novel series of carbazole-quinoline derivatives are synthesized and utilized as bipolar host materials for orange and red PhOLEDs. A record-high efficiency orange device with EQE of 25.6% and power efficiency 68.1 lm W^{-1} is achieved. These devices show very low efficiency roll-off and long operational lifetime due to the balanced charge injection in the emitting layer of the devices.